Intraseasonal Variability of the Ocean: Impacts of the Madden-Julian Oscillation

Jacob I. Rose, Bradford S. Barrett, Alexander R. Davies
Oceanography Department, U.S. Naval Academy

Research Objective: Deep tropical convection associated with the MJO forces poleward propagating upper atmospheric Rossby waves that project onto the surface as anomalies in mean sea level pressure. The resulting changes in surface pressure force surface winds, which in turn impact ocean surface currents and upwelling along the Pacific Northwest coast via Ekman dynamics.

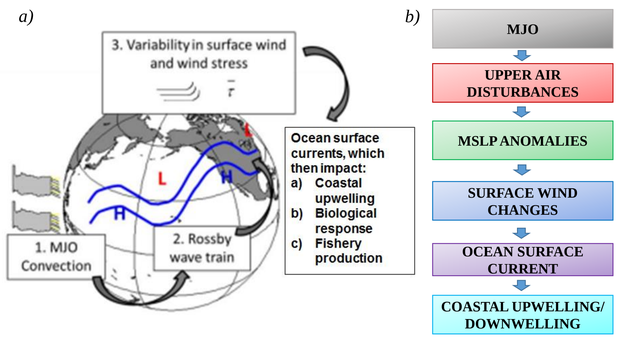

Figure 1. *a)* Proposed mechanisms supporting the research objective (adapted from Barrett et al. 2016). *b)* Mechanisms by which the MJO could potentially influence ocean currents and upwelling along the Northwest coast of North America.

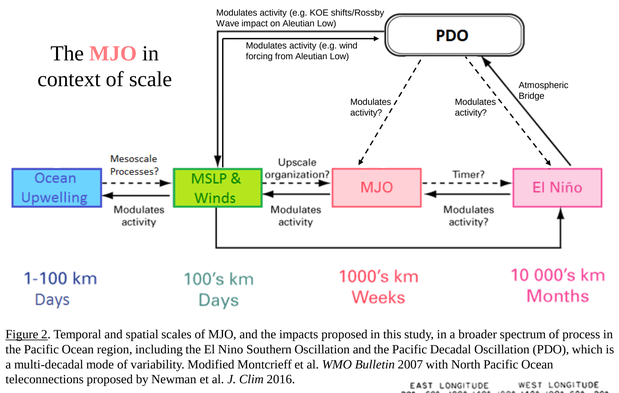

Figure 2. Temporal and spatial scales of MJO, and the impacts proposed in this study, in a broader spectrum of process in the Pacific Ocean region, including the El Nino Southern Oscillation and the Pacific Decadal Oscillation (PDO), which is a multi-decadal mode of variability. Modified Montcrieff et al. *WMO Bulletin* 2007 with North Pacific Ocean teleconnections proposed by Newman et al. *J. Clim* 2016.

Background

Madden-Julian Oscillation (MJO) is a large-scale, eastward moving envelope of strong convective thunderstorms and precipitation, which is often termed the active phase, flanked to both east and west by regions of weak convection and precipitation known as "inactive" or "suppressed" phases (Zhang, 2005). These two phases are connected by east-west zonal circulations that extend from the surface to the top of the troposphere (Figure 3), and move eastward at 5m s^{-1} (Hendon and Salby 1994).

The MJO impacts global atmospheric weather patterns on intraseasonal timescales via upper atmospheric teleconnections. This phenomena was clearly shown in studies by Hoskins and Karoly, 1981 and Sardeshmukh and Hoskins, 1988 who initialized global atmospheric models with an upper air heat source near the equator (simulating latent heat release associated with deep MJO convection). The modeling results are shown in Figures 4a and 4b and illustrate a possible upper tropospheric wave train forced by deep tropical convection associated with the MJO.

Upper air waves are the primary forcing mechanisms for synoptic scale atmospheric patterns via quasi-geostrophic theory and the locations of areas of high and low pressure at the surface (Carlson 2012). The surface pressure field drives atmospheric wind patterns via the pressure gradient force, which in turn impacts surface ocean currents through Ekman dynamics (Ekman 1905). Along the coast, Ekman transport perpendicular to the coast often results in upwelling and downwelling via conservation of mass (Mann and Lazier 2006).

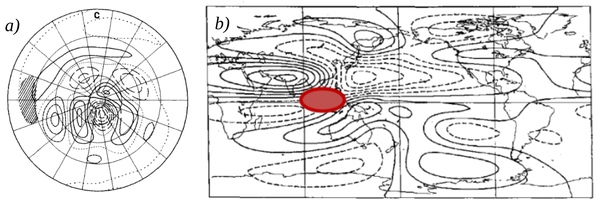

Figure 4. *a)* 300 mb height field response in to a heat source (shaded region simulating MJO convective latent heat release) in a batotropic global model (Hoskins and Karoly *JAS*, 1981). The solid lines show positive height field anomalies, dotted lines show zero height field anomalies, and dashed lines show negative height field anomalies. *b)* Theoretical equivalent barotropic wave train streamfunction at 300 mb resulting from an equatorial heat source (red oval) similar to the MJO (adapted from Sardeshmukh and Hoskins 1988). Positive stream function anomalies are shown by solid lines; negative anomalies are shown by dashed lines.

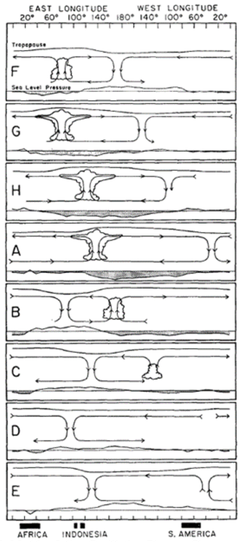

Figure 3. Madden Julian Oscillation Phases. Shown are the distinct phases along with their impact on upper troposphere heights and sea level pressures due to central convective cell heating and upward motion (e.g., in phase G the convection increases upper troposphere heights above the cell). Phases show eastward propagation across the Pacific Ocean. Image from Madden and Julian [1972].

Methods

For this study, 300mb heights (m), mean sea level pressure (MSLP; mb), and the *u* and *v* components of the 10-m wind field (m s^{-1}) were analyzed. These data were downloaded from the European Center for Medium Range Weather Forecasting (ECMWF) Reanalysis (ERA-Interim) data product available at http://www.ecmwf.int/en/research/climate-reanalysis/era-interim. All data were downloaded at 2.5° resolution between the months of November and March from 1980 to 2015. These data ranges were selected to give a statistically significant sampling record with months that aligned with the strongest MJO phases. MJO phases were determined by the Bureau of Meteorology and their Real-Time Multivariate MJO Index (RMM; Wheeler and Hendon, 2004). Data were binned and arranged by the RMM phase similar to the method of Barrett et al. (2012). Data anomalies for a given phase were calculated by subtracting the data record average for a given variable (e.g. all MSLP data in November-March from 1980-2015) from each of the RMM phase averages for a given data record. The schematic below illustrates this process (Figure 5). Number of days in each phase are also as follows: Phase 1 (*n*=335) Phase 2 (*n*=408) Phase 3 (*n*=513) Phase 4 (*n*=443) Phase 5 (*n*=409) Phase 6 (*n*=497) Phase 7 (*n*=516) Phase 8 (*n*=408).

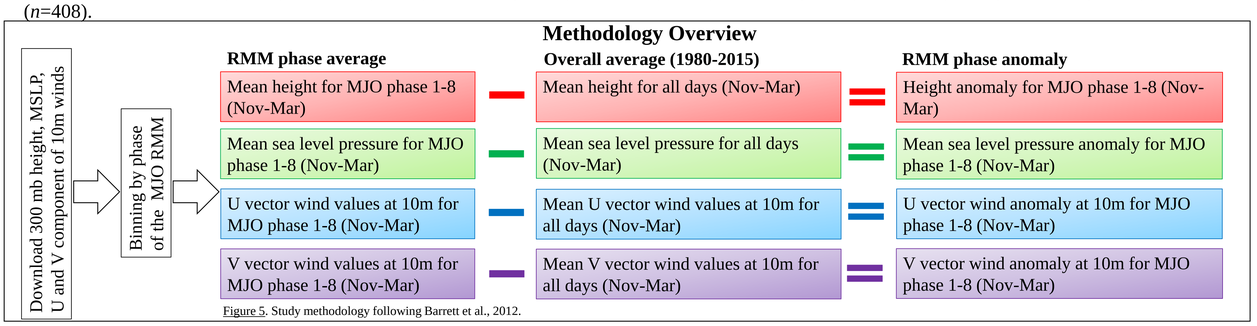

Figure 5. Study methodology following Barrett et al., 2012.

Result 1: For this analysis, the *v* vector components of the 10-m wind field were examined due to their proposed impact on coastal upwelling and downwelling along the northwest coast of North America (Mann and Lazier 2006). Phases 3 and 7 of the RMM Index were chosen for closer examination because of their polarity on the RMM phase diagram (Wheeler and Hendon, 2004), the close proximity of *v* wind anomalies to the Pacific Northwest coast (i.e. higher probability of impacting on coastal upwelling and downwelling), and because of the overall synoptic signature across the Northeast Pacific Ocean during those phases (Fig. 6).

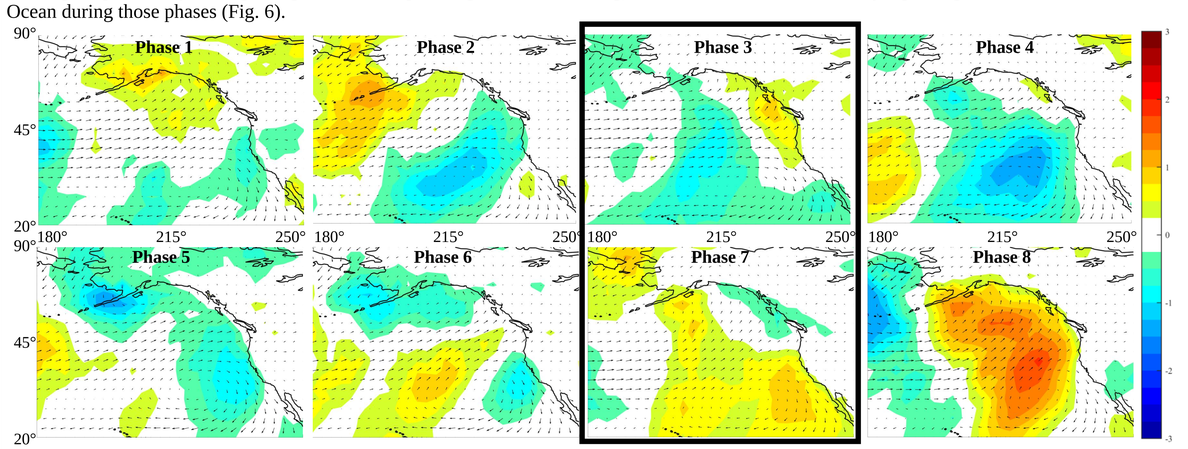

Figure 6. *v* wind vector anomalies for MJO phases 1-8. *v* vector wind anomalies are contoured with the RMM phase average wind field plotted.

Result 2: Figure 7a shows the 300mb height field anomaly during MJO phase 3. The key features are a ridge extending eastward from Japan midway through the Pacific Ocean with a trough immediately over Alaska. This is reflected in the sea level pressure anomaly (Figure 7b) as an anomalously deep Aleutian low across Alaska extending into Canada, and higher than average pressure levels across the central North Pacific basin. The resulting clockwise air flow around the high pressure system and counterclockwise air flow around the low pressure system leads to an increased westerly wind over the Pacific Ocean around 45ºN. The airflow then reaches the coast and separates, giving an anomalously faster northward winds north of 45ºN with anomalously faster southward flowing winds to the south. The expected result would be increased downwelling to the north and increased upwelling to the south via Ekman dynamics and conservation of mass.

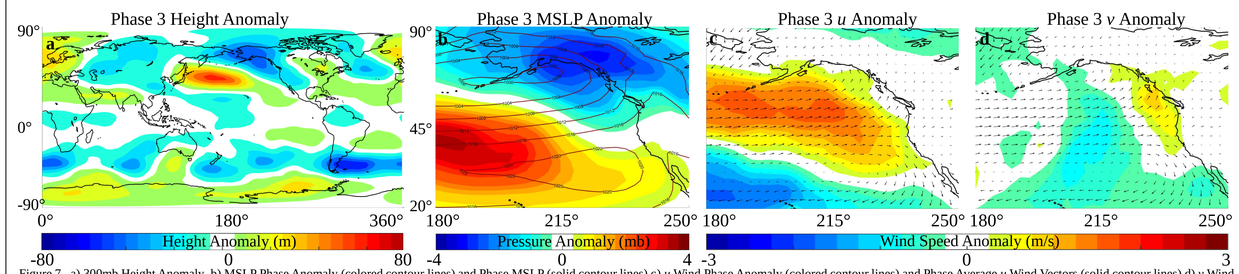

Figure 7. a) 300mb Height Anomaly b) MSLP Phase Anomaly (colored contour lines) and Phase MSLP (solid contour lines) c) *u* Wind Phase Anomaly (colored contour lines) and Phase Average *u* Wind Vectors (solid contour lines) d) *v* Wind Phase Anomaly (colored contour lines) and Phase Average *v* Wind Vectors solid contour lines for MJO Phase 3

Result 3: Figure 8a shows the 300mb height field anomaly during MJO phase 7. The main features are a trough extending from Japan nearly to the coast of California and a ridge over the center of Alaska. This is reflected in the sea level pressure anomaly (Figure 8b) as an anomalously strong low pressure system over the north Pacific and a high pressure system over Alaska extending into Canada. The resulting clockwise air flow around the high pressure system and counterclockwise air flow around the low pressure system leads to decreased (increased) westerly wind across the north Pacific Ocean north (south) of 45ºN. The airflow reaches the coast with little zonal velocity and does not spread apart as much as when compared with phase 3. During Phase 7, the southerly winds to the north of 45°N appear weaker than normal, while the northerly wind south of 45°N are anomalously strong The expected result would be decreased downwelling to the north and decreased upwelling to the south via Ekman dynamics.

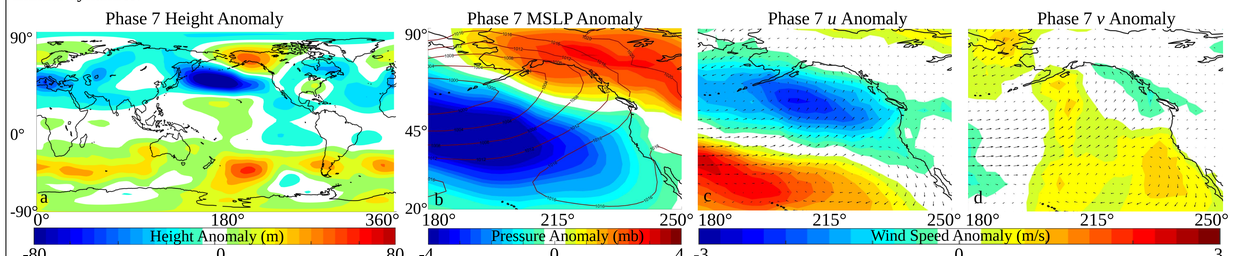

Figure 8. As with Figure 7 for MJO Phase 7

References:

Zhang, C., 2005, Madden-Julian Oscillation. *Reviews of Geophysics*, vol.**43**, no.2.
Hoskins, B., Karoly, D., 1981, The Steady Linear Response of a Spherical Atmosphere to Thermal and Orographic Forcing. *U.K. Universities' Atmospheric Modelling Group and Department of Meteorology*
Sardeshmukh, P., Hoskins, B., 1988, The Generation of Global Rotational Flow by Steady Idealized Tropical Divergence. *European Centre for Medium-range Weather Forecasts and Department of Meteorology, University of Reading*
Carlson, T., 2012: *Mid-Latitude Weather Systems*.
Ekman, V., 1905, On the Influence of the Earth's Rotation on Ocean-Currents. *Arkiv För Matematik, Astronomi Och Fysik*, Band.**2**, No.11
Mann, K., Lazier, J., 2006: *Dynamics of Marine Ecosystems Third Edition*. Blackwell Publishing.
Barrett, B., Carrasco, J., Testino, A., 2012, Madden-Julian Oscillation (MJO) Modulation of Atmospheric Circulation and Chilean Winter Precipitation. *Journal of Climate*, Vol. **25**
Wheeler, M., Hendon, H., 2004, An All-Season Real-Time Multivariate MJO Index: Development of an Index for Monitoring and Prediction. *Bureau of Meteorology Research Centre*

Acknowledgements:
The authors gratefully acknowledge financial support from NASA award NNX16AH61G.